Effect of the domain shape on noncollinear second-harmonic emission in disordered quadratic media

Mousa Ayoub,[1] Markus Paßlick,[1] Kaloian Koynov,[2] Jörg Imbrock,[*,1] and Cornelia Denz[1]

[1]*Institute of Applied Physics and Center for Nonlinear Science (CeNoS), Westfälische Wilhelms-Universität Münster, Corrensstraße 2, 48149 Münster, Germany*

[2]*Max-Planck Institute for Polymer Research, Ackermannweg 10, 55128 Mainz, Germany*

[*]*imbrock@uni-muenster.de*

Abstract: We study the role of the individual ferroelectric domain shape on the second-harmonic emission in strontium barium niobate featuring a random quadratic nonlinearity. The noncollinearly emitted second-harmonic signal is scanned in the far-field at different incident angles for different domain size distributions. This offers the possibility to retrieve the Fourier spectrum, corresponding to the spatial domain distribution and domain shape. Based on images of the domain structures retrieved by Čerenkov-type second-harmonic microscopy, domain patterns are simulated, the second-harmonic intensities are calculated, and finally compared with the measurements.

OCIS codes: (190.0190) Nonlinear optics; (190.4410) Nonlinear optics, parametric processes; (190.4975) Parametric processes; (160.2260) Ferroelectrics.

References and links

1. A. R. Tunyagi, M. Ulex, and K. Betzler, "Noncollinear optical frequency doubling in strontium barium niobate," Phys. Rev. Lett. **90**, 243901 (2003).
2. R. Fischer, D. N. Neshev, S. M. Saltiel, A. A. Sukhorukov, W. Krolikowski, and Y. S. Kivshar, "Monitoring ultrashort pulses by transverse frequency doubling of counterpropagating pulses in random media," Appl. Phys. Lett. **91**, 031104 (2007).
3. V. Roppo, D. Dumay, J. Trull, C. Cojocaru, S. M. Saltiel, K. Staliunas, R. Vilaseca, D. N. Neshev, W. Krolikowski, and Y. S. Kivshar, "Planar second-harmonic generation with noncollinear pumps in disordered media," Opt. Express **16**, 14192–14199 (2008).
4. J. Trull, C. Cojocaru, R. Fischer, S. M. Saltiel, K. Staliunas, R. Herrero, R. Vilaseca, D. N. Neshev, W. Krolikowski, and Y. S. Kivshar, "Second-harmonic parametric scattering in ferroelectric crystals with disordered nonlinear domain structures," Opt. Express **15**, 15868–15877 (2007).
5. V. Roppo, W.Wang, K. Kalinowski, Y. Kong, C. Cojocaru, J. Trull, R. Vilaseca, M. Scalora, W. Krolikowski, and Y. Kivshar, "The role of ferroelectric domain structure in second harmonic generation in random quadratic media," Opt. Express **18**, 4012–4022 (2010).
6. M. Ayoub, J. Imbrock, and C. Denz, "Second harmonic generation in multi-domain χ^2 media: from disorder to order," Opt. Express **19**, 11340–11354 (2011).
7. L. Tian, D. A. Scrymgeour, and V. Gopalan, "Real-time study of domain dynamics in ferroelectric $Sr_{0.61}Ba_{0.39}Nb_2O_6$," J. Appl. Phys. **97**, 114111 (2005).
8. K. Terabe, S. Takekawa, M. Nakamura, K. Kitamura, S. Higuchi, Y. Gotoh, and A. Gruverman, "Imaging and engineering the nanoscale-domain structure of a $Sr_{0.61}Ba_{0.39}Nb_2O_6$ crystal using a scanning force microscope," Appl. Phys. Lett. **81**, 2044–2046 (2002).

#197824 - $15.00 USD Received 17 Sep 2013; revised 8 Nov 2013; accepted 8 Nov 2013; published 13 Dec 2013

9. M. Ayoub, P. Roedig, J. Imbrock, and C. Denz, "Domain-shape-based modulation of Čerenkov second-harmonic generation in multidomain strontium barium niobate," Opt. Lett. **36**, 4371–4373 (2011).
10. J. Bravo-Abad, X. Vidal, J. L. D. Juárez, and J. Martorell, "Optical second-harmonic scattering from a non-diffusive random distribution of nonlinear domains," Opt. Express **18**, 14202–14211 (2010).
11. M. Ayoub, P. Roedig, K. Koynov, J. Imbrock, and C. Denz, "Čerenkov-type second-harmonic spectroscopy in random nonlinear photonic structures," Opt. Express **21**, 8220–8230 (2013).
12. Y. Sheng, A. Best, H.-J. Butt, W. Krolikowski, A. Arie, and K. Koynov, "Three-dimensional ferroelectric domain visualization by Čerenkov-type second harmonic generation," Opt. Express **18**, 16539–16545 (2010).
13. S. M. Russell, P. E. Powers, M. J. Missey, and K. L. Schepler, "Broadband mid-infrared generation with two-dimensional quasi-phase-matched structures," J. Quantum Electronics **37**, 877–887 (2001).
14. A. Arie and N. Voloch, "Periodic, quasi-periodic, and random quadratic nonlinear photonic crystals," Laser and Photon. Rev. **4**, 355–373 (2010).
15. K. Kalinowski, P. Roedig, Y. Sheng, M. Ayoub, J. Imbrock, C. Denz, and W. Krolikowski, "Enhanced Čerenkov second-harmonic emission in nonlinear photonic structures," Opt. Lett. **37**, 1832–1834 (2012).

1. Introduction

Random nonlinear photonic crystals (RNPCs) have attracted significant interest in recent years due to their potential benefits for broadband second-harmonic generation (SHG) and ultrashort pulse monitoring [1–3]. The randomness is characterized by the random size and spatial position distribution of ferroelectric domains, which represent the $\chi^{(2)}$ nonlinearity in the ferroelectrics. Consequently, such a structure enables phase matching of various parametric processes over an ultra-broad spectral range and in different spatial directions transverse to the beam propagation [4–6]. An example of a quadratic nonlinear medium with randomized domain structures is an unpoled strontium barium niobate (SBN) crystal. Such a crystal shows an intrinsic 2D disordered domain structure. The ferroelectric domains have the form of rods with a shape of fourfold symmetry. The domain cross-sections are squares with rounded corners [7]. The averaged domain sizes reported in the literature range from tens of nanometers to a few micrometers [8, 9] [see Figs. 1(a) and 1(b)]. The effect of this shape on the Čerenkov-type SH intensity in random SBN has been studied in a number of publications [9,10]. It was experimentally demonstrated that the emitted patterns become fourfold modulated and the modulation is more pronounced for microscaled domains [9]. However, up to now the effect of the domain shape in random nonlinear photonic structures on the noncollinear planar SH pattern was not explained.

In this paper, we investigate both experimentally and theoretically the effect of the domain shape in an SBN crystal on the noncollinear planar second-harmonic generation in the far-field. Theoretically, while the single-domain model showed the ability to describe the fourfold modulation of the Čerenkov cone [9, 10], the noncollinear planar second-harmonic generation leads to a two-dimensional domain distribution, the key clarifying this broadband conversion process.

2. Experimental methods

In order to illustrate the role of the domain shape, we will distinguish between two characteristic averaged domain sizes, corresponding to two characteristic poling states; the unpoled case or "as-grown", in which the averaged domain size is about $200-300$ nm [6,11] [see Fig. 1(a)] and, the repoled case, in which the averaged domain size is about $3-5$ μm [6, 11] [see Fig. 1(b)]. The images depicted in Figs. 1(a) and 1(b) were obtained by Čerenkov-type second-harmonic generation microscopy, described in details elsewhere [12]. In the experiment, the planar SH emission [see Fig. 1(c)] is scanned for the two cases and for different angles of incidence of the fundamental beam in order to map the Fourier spectrum, which represents the spatial domain distribution and the domain shape. The corresponding phase-matching condition is illustrated in Fig. 1(d). In Fig. 1(e), a schematic illustration of the experimental setup for measuring the an-

#197824 - $15.00 USD Received 17 Sep 2013; revised 8 Nov 2013; accepted 8 Nov 2013; published 13 Dec 2013

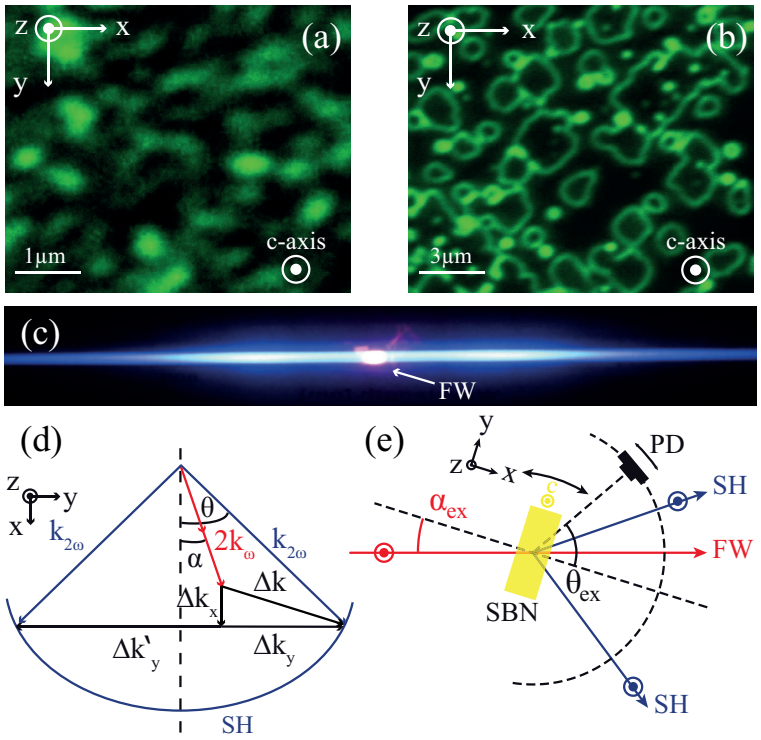

Fig. 1. Disordered ferroelectric domain patterns in as-grown (a) and repoled (b) strontium barium niobate imaged by scanning Čerenkov-type SHG microscopy; (c) An experimental photograph of planar SH at 400 nm for a repoled sample, corresponding to an averaged domain size shown in (b); (d) Phase-matching condition diagram; (e) Schematic illustration of the experimental setup.

gular second-harmonic intensity is shown. As a light source, we use ultrashort laser pulses, generated by a laser system consisting of a mode-locked Ti:sapphire oscillator, and a regenerative amplifier. The repetition rate is 1 kHz, the pulse duration is about $\tau_p = 100$ fs, and the pulse energy amounts to 150 μJ at the wavelength 800 nm which is used in the experiments. Collimated Gaussian laser pulses with a beam diameter of about 2.5 mm are propagating in the *xy*-plane of the SBN crystal. The light is always extraordinarily polarized. A $Sr_{0.61}Ba_{0.39}Nb_2O_6$ sample with the dimensions $3.5 \times 3.5 \times 1$ mm^3 is employed. The large surfaces parallel to the *c*-axis are polished to optical quality. The SBN sample is mounted on a rotation stage which allows us to control the incident angle α_{ex}. The SH intensity is measured using a silicon photo diode mounted on another rotation stage centered around the crystal in the *xy*-plane [see Fig. 1(e)]. Both rotation stages have the same rotating axis. In preparation, the crystal was first heated up above the Curie temperature $T_c \approx 70\,^{\circ}$C, and then cooled down without applying an electric field to produce a state similar to an as-grown sample. In order to influence the domain size, the sample was subsequently poled and repoled stepwise at room temperature with the same procedure shown in [6]. For this purpose, an electric field was applied along the polar axis and increased in steps of 10 V every 2 s above the coercive field until finally 7.5 kV/cm are reached. To repole the crystal the direction of the electric field was reversed and increased as it was applied in one direction to pole the crystal and vice versa to repole it.

#197824 - $15.00 USD Received 17 Sep 2013; revised 8 Nov 2013; accepted 8 Nov 2013; published 13 Dec 2013

3. Numerical simulations

Figure 2 illustrates the idea of the measurements performed in this paper. It demonstrates two

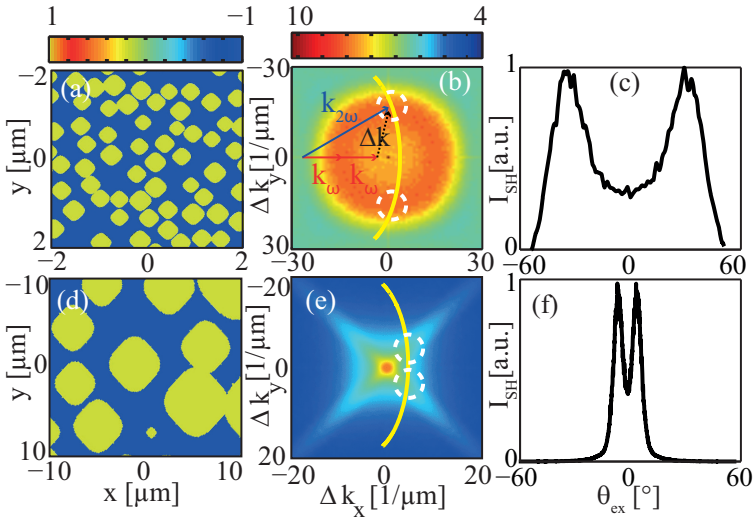

Fig. 2. (a, d) Modeled real space of random up- and down-domain structure for the two averaged domain sizes of 0.25 µm and 3.5 µm, respectively; (b, e) The corresponding Fourier spectra. The strongest Fourier coefficients are marked with dashed white circles; (c, f) Calculated SH angular intensity for the two domain distributions for a fundamental wavelength of 800 nm.

numerical simulations of two 2D domain distributions. The two domain widths are Gaussian distributed with the mean values 0.25 µm with a standard deviation of 0.07 µm and 3.5 µm with a standard deviation of 0.7 µm, respectively (Figs. 2(a) and 2(d)). The simulated domains are of square shape with rounded corners, so called *squircles*, and the shape of the domains can be described by the following equation:

$$s^2 \frac{x^2 y^2}{r_D^4} - \left(\frac{x^2}{r_D^2} + \frac{y^2}{r_D^2} \right) + 1 = 0 \,. \tag{1}$$

Here, s is the degree of the squareness. The domain is of square shape when $s = 1$ and of circular shape when $s = 0$. The domain radius is denoted by r_D. All domains are rotated by 45° with respect to the *xy*-coordinates in order to mimic the microscopic image Fig. 1(b). Please note that the orientation of the domains in one specific sample is fixed while the orientation might be different in other samples depending on the particular crystal cut. In Figs. 2(b) and 2(e), the corresponding Fourier spectra are shown. For nanoscaled domains [Fig. 2(a)], the Fourier spectrum is circularly shaped [Fig. 2(b)]. The radius of the circle is directly related to the mean domain size and its width is related to the standard deviation. The individual domain shape has no significant effect on the circle symmetry for nanoscaled domains. In contrast, for microscaled domains [Fig. 2(d)], the strongest Fourier coefficients shift to smaller spatial frequencies and the individual domain shape is more pronounced through the four tails [Fig. 2(e)]. In consequence, different SH patterns and dependencies are expected. As well known, the SH intensity is proportional to the square of the Fourier coefficients [13–15]. For a two-dimensional

#197824 - $15.00 USD Received 17 Sep 2013; revised 8 Nov 2013; accepted 8 Nov 2013; published 13 Dec 2013

(2D) $\chi^{(2)}$ structure modulated in the *xy*-plane the SH intensity is

$$I_{\mathrm{SH}} \propto d_{\mathrm{eff}}^2 I_{\mathrm{FW}}^2 L_z^2 |S(\Delta k_x, \Delta k_y)|^2 \mathrm{sinc}^2\left(\frac{\Delta k_z L_z}{2}\right), \tag{2}$$

where I_{FW} is the intensity of the fundamental wave propagating along the *x*-axis, L_z is the domain length, and $S(\Delta k_x, \Delta k_y)$ is the Fourier spectrum of the domain structure with the transverse phase mismatch vectors $\Delta k_x = k_{2\omega}\cos(\theta) - 2k_\omega \cos(\alpha)$, and $\Delta k_y = k_{2\omega}\sin(\theta) - 2k_\omega \sin(\alpha)$ in the *x*- and *y*-direction, respectively [see Fig. 1(d)]. To determine the relevant Fourier coefficients, the phase-matching condition is applied to the spectra for the fundamental beam with a wavelength of 800 nm [see Fig. 2]. The strongest Fourier coefficients are marked with dashed circles. As it is clearly seen, different SH intensity patterns are expected for both cases. According to Eq. 2, Figs. 2(c) and 2(f) show the calculated SH intensity distributions, which correspond to the Fourier spaces in Figs. 2(b) and 2(e), respectively. The Figs. clearly show intensity peaks with different widths at different emission angles. It is worth to note here, that with increasing the fundamental wavelength the participated Fourier coefficients shift to smaller spatial frequencies in both cases. However, the calculated SH peaks will show different tendency, in which they move out to larger emission angles for nanoscaled domains, in contrast to microscaled case, corresponding to the measured data in [6].

4. Experimental results and discussion

In order to prove the effect of the domain shape on the SH intensity, the sample is rotated and the SH intensity is measured. The second-harmonic intensity distribution in Fig. 2(c) exhibits no change except that caused by the reflection at the inner faces, because the spectrum is symmetric. The result is depicted in Fig. 3(a). With respect to the fundamental beam, marked by

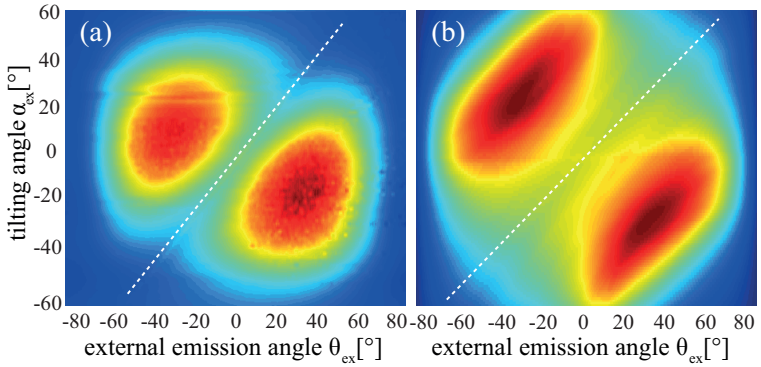

Fig. 3. (a) Experimentally measured SH signal at 400 nm while rotating the unpoled SBN sample; (b) Simulated SH intensity as a function of the incident and emission angles (Media 1). The fundamental beam direction is marked with a dashed line.

a dashed white line, the scan shows identical peaks for the entire tilting region corresponding to the numerical simulations [cf. Fig. 3(b)]. For the asymmetric spectrum, i.e. microscaled domains, the result is depicted in Fig. 4(a). The two SH peaks are symmetric for normal incidence but they become asymmetric with respect to the fundamental beam when starting to rotate the sample. Numerically, the SH intensity is calculated for three different squareness degrees s = 0.4, 0.6, and 0.8. The calculations are performed for the averaged domain width 3.5 μm. Figure 4(b) indicates only one peak in the middle at normal incidence. When increasing the squareness to s = 0.6 [Fig. 4(c)], the SH intensity peak at normal incidence splits into two peaks.

#197824 - $15.00 USD Received 17 Sep 2013; revised 8 Nov 2013; accepted 8 Nov 2013; published 13 Dec 2013

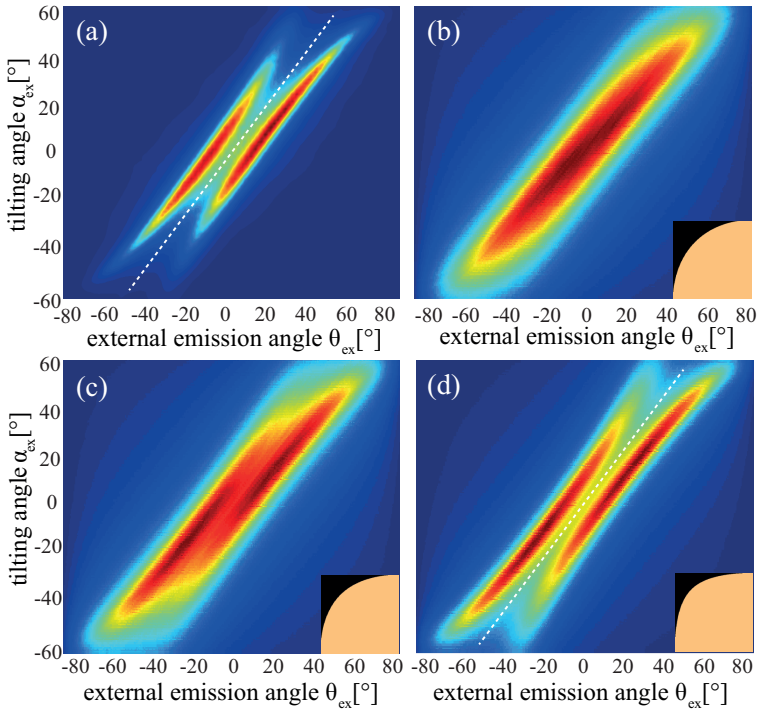

Fig. 4. (a) Experimentally measured SH signal at 400 nm while rotating the repoled SBN sample (Media 2); (b, c, d) Simulated SH intensity as a function of the incident and emission angles for the squareness degrees $s = 0.4, 0.6, 0.8$, respectively. The insets show the corresponding modeled domain shape. The fundamental beam direction is marked by a dashed line.

The peaks become more distinct for s = 0.8 in [Fig. 4(d)]. In agreement with the measurements, the calculated SH intensity clearly shows the asymmetry in the SH intensity at both sides when starting to rotate the sample. The SH intensity increases with decreasing negative incident angle, indicating an inhomogeneous distribution of the Fourier coefficients. This behavior confirms the role of the domain shape in forming the SH pattern in the far-field. The best agreement between the numerical simulations and the experimental measurements is achieved for a squareness degree of the domains of $s = 0.8$. This domain shape of a square with rounded corners is also visible in the microscopic image in Fig. 1(b) when one compares it with the inset of Fig. 4(d). However, it is hard to determine an exact parameter s directly from Fig. 1(b) because often domains merge inside the crystal. Furthermore, all domain parameters like the width, variance, and domain shape that are deduced from the experimental results are statistical parameters averaged over a large number of domains.

The presented method of scanning the second-harmonic intensity in the far-field can be in principle used to determine the statistical domain parameters of the random nonlinear photonic structure. It works in a similar way as the recently published method of Čerenkov-type second-harmonic spectroscopy [11] using the so-called conical geometry. However, the calculation of the domain parameters from the far-field second-harmonic intensity distribution is an inverse scattering problem and the retrieved Fourier spectra might be in general ambiguous. Therefore, to get reliable parameters one needs in addition further information about the order of the domain parameters which are accessible for instance by Čerenkov-type second-harmonic

#197824 - $15.00 USD Received 17 Sep 2013; revised 8 Nov 2013; accepted 8 Nov 2013; published 13 Dec 2013

microscopy.

In our nonlinear photonic structure the position of each individual domain is random and the domain diameters also vary randomly. However, the orientation of each domain is fixed due to the crystal symmetry. Hence, the fixed domain orientation and the characteristic domain shape always lead to a fourfold modulated Fourier spectrum and therefore to a spatially modulated second-harmonic signal whenever the mean domain diameter is larger than the second-harmonic wavelength. Thus, the influence of the domain orientation and shape on the second-harmonic intensity distribution should also be visible in other random nonlinear photonic structures exhibiting a disordered domain structure. For instance a threefold modulated second-harmonic intensity distribution is expected in random lithium niobate crystals due to the hexagonal domain shape.

5. Conclusions

In conclusion, we demonstrated experimentally and numerically the influence of the individual domain shape on the second-harmonic emission in random nonlinear photonic structures. Experimentally, an SBN crystal, whose domain structures are of square shape with rounded corners, was taken as a platform to create different domain size distributions. We showed that for nanoscaled domains the effect of the domain shape is not observable, while it is more pronounced for microscaled domains. The far-field second-harmonic intensity distribution can be perfectly simulated using a two-dimensional Fourier spectrum of the random domain pattern. Especially the modulated second-harmonic intensity distribution created by nanoscaled domains cannot be described by a single-domain model because a single domain would always lead to a maximum in the second-harmonic intensity in the direction of the fundamental wave. The combination of Čerenkov-type second-harmonic microscopy and far-field second-harmonic intensity scanning is well suited to analyze a variety of random as well as periodic nonlinear photonic structures.

Acknowledgment

Financial support of Deutsche Forschungsgemeinschaft and Open Access Publication Fund of University of Münster is gratefully acknowledged.

#197824 - $15.00 USD Received 17 Sep 2013; revised 8 Nov 2013; accepted 8 Nov 2013; published 13 Dec 2013